Journal of Oceanography, Vol. 57, pp. 603 to 616, 2001

Dependence of Whitecap Coverage on Wind and Wind-Wave Properties

DONGLIANG ZHAO[1,2]* and YOSHIAKI TOBA[1,3]

[1]*Earth Observation Research Center, National Space Development Agency of Japan, Tokyo 104-6023, Japan*
[2]*Institute of Physical Oceanography, Ocean University of Qingdao, Qingdao 266003, China*
[3]*Research Institute for Environmental Sciences and Public Health of Iwate Prefecture, Morioka 020-0852, Japan*

(Received 6 November 2000; in revised form 23 April 2001; accepted 28 April 2001)

Using Phillips equilibrium range theory and observational data, we show first that the total rates of wave energy dissipation estimated by the Hasselmann and Phillips dissipation models are substantially consistent with each other, though their original forms are different. Both are proportional to the cube of air friction velocity, u_*^3, with a weak dependence on wave age. As a direct manifestation of the wave energy dissipation processes, we reanalyze previous observational data of whitecap coverage and find that it has greater correlation with the wind speed or friction velocity than the wave period or wave age. However, the data scatter decreases remarkably when the breaking-wave parameter $R_B = u_*^2/\nu\omega_p$ is used, where ν is the kinematic viscosity of air, and ω_p the wind-wave spectral peak frequency. Physical interpretation of R_B with some related issues, and a discussion of the probability models of whitecap coverage in terms of a threshold mechanism, are also presented. We conclude that R_B is a good parameter to effectively express the overall wave breaking behavior for the case of wind-waves in local equilibrium with the wind. Since R_B can be expressed as the product of u_*^3 and the wave age, this result demonstrates a stronger dependence of whitecap coverage on wave age than expected by the previous description by power-laws of u_* and by the two theoretical models. Our conclusion suggests that current dissipation models should also be modified to represent full properties of wind-wave breaking.

Keywords:
· Wind-waves,
· energy dissipation,
· wave breaking,
· whitecap coverage,
· breaking-wave parameter.

1. Introduction

Breaking waves in deep water are closely involved in a number of processes at the air-sea boundary. These include the horizontal stress exerted by the wind, the energy dissipation of surface waves, the vertical mixing in the upper ocean, the exchange of heat and gases, and the generation of aerosols by bursting bubbles. Wave breaking is a highly nonlinear process and its quantitative estimation is very difficult, both experimentally and theoretically.

Recent wave models have attempted to predict the full directional wave spectrum based on the numerical solution of the radiative transfer equation (e.g., WAMDI Group, 1988). The source terms, including the wind input, nonlinear wave-wave interactions and wave dissipative processes, have been synthesized both from observational and theoretical results. Of these, the dissipation source term is the least understood. The dissipation of wave energy is believed to be dominated by wave breaking or whitecapping, the form of which is at present not known exactly from observations. Hasselmann (1974) proposed a theoretical model based on the proposition that the wave breaking is weak on average and is quasi-linear in the spectral density. Phillips (1985) argued that wind-wave breaking needs to be a nonlinear function of the spectral density. The Hasselmann model has been adopted widely, both in model studies and in operational wave models, with apparent success (WAMDI Group, 1988), while the Phillips model has been supported by some acoustic studies of wind-wave breaking (Kennedy, 1992; Felizardo and Melville, 1995).

* Corresponding author. E-mail: zhao@eorc.nasda.go.jp

Whitecaps are a well-known surface signature of breaking wave and air entrainment processes. Whitecap coverage is another way to quantitatively evaluate the breaking of wind-waves, and many studies have focused on it. From the pictures of whitecaps taken by camera or video recorder, whitecap coverage is obtained by evaluating the white part of the total area of the picture. In place of a detailed physical representation of breaking waves, empirical models typically employ wind speed expressions to describe the wave-induced effects. For example, by using the data of Monahan (1971) and Toba and Chaen (1973), Wu (1979) proposed a clear power-law dependence on wind forcing of the form:

$$W \sim u_*^3 \sim U^{3.75} \tag{1}$$

where W is the whitecap coverage of the sea surface, u_* the air friction velocity, and U is the wind speed at 10-m elevation. Wu (1979, 1982) emphasized that his conclusions were not merely derived from curve fitting, but the exponent was obtained from the consideration of the energy flux from wind to waves. However, Monahan and O'Muircheartaigh (1980, 1982) expressed reservations about this 3.75 power law and presented their own power law descriptions.

Very few attempts have been made to augment or replace wind speed with wave parameters in air-sea modeling. Using modeled wave spectra, Cardone (1970) found that W, as observed by Monahan (1969) on the fresh water Great Lakes, is better correlated with theoretical energy dissipation estimates than with wind speed alone. Toba and Koga (1986) suggested a dimensionless parameter

$$R_B = u_*^2 / \nu\omega_p \tag{2}$$

where ν is the kinematic viscosity of air and ω_p is the peak angular frequency of wind-waves, which can be widely used to describe the overall conditions of air-sea boundary processes. R_B will be called the breaking-wave parameter hereafter, following the nomenclature of Toba *et al.* (1999). They also assigned a critical value of $R_B = 10^3$ for the onset of wind-wave breaking. Hanson and Phillips (1999) estimated the total rate of wave energy dissipation D_t from the Gulf of Alaska observations based on the Phillips dissipation model. They found a good correlation between whitecap coverage and D_t.

Another approach to the quantitative estimation of the wave-breaking process is the probability model that evaluates whitecap coverage in terms of a threshold mechanism. This model was first proposed by Snyder *et al.* (1983). Due to the practical difficulties in determining the wave breaking criterion and the high order moment of the wind-wave spectrum, a definite expression of W is usually not available for this method (Xu *et al.*, 2000).

In Section 2, as a preliminary consideration for whitecap coverage studies, we try to express the total rate of wave energy dissipation based on two dissipation models proposed by Hasselmann (1974) and Phillips (1985), using the concept of the Phillips (1985) equilibrium range theory and field observations. Then, in Section 3, we reanalyze previous observational data of whitecap coverage that include wind-wave information, by the method of least squares. The results show a stronger dependence of whitecap coverage on wave age than expected from traditional form such as Eq. (1), and the superiority of the breaking-wave parameter R_B. Probability models for whitecap coverage are also discussed in detail in Section 4. In Section 5 we then discuss the physical interpretation of R_B. Section 6 presents our conclusion.

2. Model Analysis for Wind-Wave Energy Dissipation

As mentioned above, there are two spectral dissipation models, the Hasselmann model and the Phillips model, which have been proposed for estimating the rate of wave energy dissipation. The former has been widely incorporated in the current numerical wave model with apparent success. One reason is that it is easy to operate in combination with other source terms having a linear dependence on spectral density. In contrast, no operational wave models have adopted the Phillips model to evaluate the wave energy dissipation because it would be too complicated due to its dependence on the cube of spectral density. However, field measurements of the acoustic dipole source intensity (Kennedy, 1992) suggest that the breaking wave acoustic spectrum is self-similar and is scaled by the friction velocity cubed, which is proportional to the rate of energy dissipation determined by the Phillips model. Felizardo and Melville (1995) also showed that correlations between the ambient noise and the surface wave dissipation estimates based on the Hasselmann and Phillips models are comparable. All of these facts induced us to investigate the two models further.

Phillips (1985) considered that the high-frequency components of the wave field (wind-waves) are essentially in equilibrium with the wind. This concurs with the field observation by Toba *et al.* (1988). By using a simplified spectral flux expression and the Plant (1982) wind input formula, Phillips (1985) showed that the equilibrium forms for the wind-wave number and frequency spectra are

$$\Psi(\vec{k}) = \delta(\cos\theta)^p u_* g^{-1/2} k^{-7/2} \tag{3}$$

$$\Phi(\omega) = \alpha u_* g \omega^{-4} \tag{4}$$

where α is the Toba constant. The value of δ is obtained from the equation $\delta = \alpha/4I(p)$, which relates to the magnitudes of the frequency and wave number spectra, and the surface wind-wave spreading function

$$I(p) = \int_{-\pi/2}^{\pi/2} (\cos\theta)^p d\theta. \tag{5}$$

Equation (4) was proposed by Toba (1973) as a self-similar high frequency spectral form, which is consistent with the 3/2-power law (shown below in Eq. (16)), also based on some observational data, and confirmed in many theoretical studies and field observations.

2.1 *Phillips' dissipation model*

The Phillips (1985) equilibrium range concepts allow us to express each source term as a function of the equilibrium range spectrum. He assumed the three source terms are proportional and comparable. The source term of wind-wave dissipation due to wave breaking is given by

$$S_{ds}(\vec{k}) = \rho_w g \gamma k^8 \Psi^3(\vec{k}) \tag{6}$$

where γ is obtained from the assumption that the wind input term is comparable to the dissipation term, with $\gamma\delta^2 \approx 0.04$. In terms of the frequency spectrum, Eq. (6) can be written as

$$S_{ds}(\omega) = \frac{\rho_w \gamma I(3p)}{16[I(p)]^3 g^3} \omega^{11} \Phi^3(\omega). \tag{7}$$

The total rate of wave energy dissipation can therefore be computed by

$$D_{pt} = \int_{\omega_p}^{\omega_1} S_{ds}(\omega) d\omega. \tag{8}$$

Substitution of Eq. (4) into Eq. (8) gives

$$D_{pt} = 4\gamma\delta^3 I(3p) \rho_w u_*^3 \int_{\omega_p}^{\omega_1} \omega^{-1} d\omega. \tag{9}$$

The integral will be infinite unless a finite upper limit ω_1 is introduced. Phillips (1985) gave this upper limit $\omega_1 = r^{1/2} g/u_*$, where r is a constant of order one. Integration of Eq. (9) and use of the lower limit $\omega_p = g/c_p$ give

$$D_{pt} = 4\gamma\delta^3 I(3p) \rho_w u_*^3 \ln\left[r^{1/2}\beta\right] \tag{10}$$

where $\beta = g/u_*\omega_p$ is a parameter representing the degree of wind-wave development, which is called wave age. The difficulty in modeling the characteristics of the directional distribution of the wave field gives some uncertainty in the Phillips dissipation estimate. Phillips (1985) showed that the lower (upper) bound of the directional spreading parameter p in Eq. (10) is 0.5 (2.0). Consequently, $\gamma\delta^3 I(3p)$ is expected to be in the range 3.7 to 8.0×10^{-4}, giving an average value of 5.9×10^{-4}. Substituting this value into Eq. (10) gives the total dissipation energy

$$D_{pt} \approx 2.36 \times 10^{-3} \rho_w u_*^3 \ln\left(r^{1/2}\beta\right). \tag{11}$$

Equation (11) suggests that the total rate of wave energy dissipation is proportional to the cube of friction velocity with a weak dependence on wave age. This weak dependence on wave age shows that wave energy dissipation becomes larger due to wave breaking as the wave age increases.

2.2 *Hasselmann's dissipation model*

In contrast, Hasselmann (1974) argued that, although the wave breaking is locally a highly nonlinear process, it is in general weak on average. To the lowest order, the spectral dissipation should be a quasi-linear function of Φ and a damping coefficient, which is proportional to the square of the frequency ω, that is

$$S_{ds}(\omega) = \rho_w g \eta \omega^2 \Phi(\omega) \tag{12}$$

where η is a constant. Komen *et al.* (1984) and the WAMDI Group (1988) proposed the following expression for the coefficient η

$$\eta = \frac{c_0}{\bar{\omega}} \left(\frac{\bar{\alpha}}{\bar{\alpha}_{PM}}\right)^2 \tag{13}$$

where $c_0 = 3.33 \times 10^{-5}$ and $\bar{\alpha}_{PM} = 4.57 \times 10^{-3}$. $\bar{\alpha} = E\bar{\omega}^4/g^2$ is a measure of wave steepness using a kind of nondimensional total wave energy, $E = \int\Phi(\omega)d\omega$ being the total surface wave energy, and $\bar{\omega} = \int\omega\Phi(\omega)d\omega/E$ being the mean frequency of the wave spectrum.

Two methods can be used to estimate the wave energy dissipation based on the Hasselmann model, depending on the method used in calculating the total wind-wave energy. One is to substitute Eq. (4) into (13) to calculate E directly. The integration range will be from ω_p to infinity. The total rate of wave energy dissipation is

$$D_{ht} = \rho_w g \frac{c_0}{\overline{\omega}} \left(\frac{\overline{\alpha}}{\overline{\alpha}_{PM}} \right)^2 \int_{\omega_p}^{\infty} \omega^2 \Phi(\omega) d\omega$$

$$= \frac{1}{9} (1.5)^7 \frac{c_0 \alpha^3}{\overline{\alpha}_{PM}^2} \rho_w u_*^3. \tag{14}$$

With the Toba's constant $\alpha = 0.09$, Eq. (14) can be written as

$$D_{ht} \approx 2.21 \times 10^{-3} \rho_w u_*^3. \tag{15}$$

With the direct calculation of E based on Eq. (4), Eq. (15) indicates that the total rate of wave energy dissipation estimated by the Hasselmann model is also proportional to the cube of wind friction velocity, as in the Phillips model, but is completely independent of wave parameters.

Another method to estimate the total wind-wave energy E in $\overline{\alpha}$ is to use the relationship between the nondimensional wind-sea energy $E^* = Eg^2/U^4$ and the wave age $g/\omega_p U$, which has been investigated in many field studies. These relationships, in historical series, can be summarized as follows

$$E^* = 0.0020 (g / \omega_p U)^{3.0}$$
$$\text{(Toba 3/2 law, 1972, 1978)} \tag{16}$$

$$E^* = 0.0017 (g / \omega_p U)^{3.0}$$
$$\text{(Mitsuyasu } et\ al.\text{, 1980)} \tag{17}$$

$$E^* = 0.0022 (g / \omega_p U)^{3.3}$$
$$\text{(Donelan } et\ al.\text{, 1992)} \tag{18}$$

$$E^* = 0.0014 (g / \omega_p U)^{3.23}$$
$$\text{(Glazman and Greysukh, 1993)} \tag{19}$$

$$E^* = 0.0020 (g / \omega_p U)^{3.22}$$
$$(U \geq 5 \text{ m/s, Hanson and Phillips, 1999}) \tag{20}$$

$$E^* = 0.0022 (g / \omega_p U)^{3.02}$$
$$\text{(all data, Hanson and Phillips, 1999).} \tag{21}$$

In Eq. (16), u_* in the original expressions has been converted to U by using the drag coefficient $C_D = 0.0015$. It is obvious that all of these equations have the same form, which can be expressed as

$$E^* = a (g / \omega_p U)^b \tag{22}$$

where b lies between 3.0 and 3.3. By estimating the total wind-wave energy E from Eq. (16), the total wave energy dissipation by wave breaking based on Hasselmann model becomes

$$D_{ht} = (1.5)^7 \frac{c_0 \alpha}{\overline{\alpha}_{PM}^2} a^2 C_D^{b-4} \rho_w u_*^3 \beta^{2b-6} \tag{23}$$

where the drag coefficient $C_D = u_*^2/U^2$ is used in the derivation. If we take C_D as a constant value of magnitude 0.0015, Eq. (23) can be approximated as

$$D_{ht} \approx 6.54 \times 10^{-3} \rho_w u_*^3 \beta^{2b-6}. \tag{24}$$

Since $b = 3.0$ to 3.3, the index of wave age β will be in the range of 0 to 0.6 with an average value of 0.3. As in the Phillips model, Eq. (24) clearly shows that the total rate of wave energy dissipation is proportional to the cube of wind friction velocity with a weak dependence on wave age. D_{ht} also increases as the wind wave develops.

The above analysis reveals that the dissipation models of Hasselmann and Phillips are substantially consistent with respect to the total rate of wave energy dissipation, though they differ significantly in form, as well as the concept of their derivation. Both show that the total rate of wave energy dissipation is proportional to the cube of air friction velocity and depends very weakly on wave age.

Whitecap coverage W is just another way to describe wave breaking quantitatively, so it should be directly proportional to the total rate of wave energy dissipation, as pointed out by Hanson and Phillips (1999). This will lead to the conclusion of $W \sim u_*^3$ that is almost independent of wave age and agrees with the power law such as expressed in Eq. (1).

3. New Analysis of Observational Data of Whitecap Coverage

Many observations of whitecap coverage have been made by taking a number of video recordings of the sea surface (e.g., Monahan and O'Muircheartaigh, 1980). The basic assumption is that, in a video picture of the sea surface, all pixels with gray levels above a certain threshold value correspond to whitecaps, and all other elements in the picture having gray levels below that threshold correspond to non-whitecap areas. As mentioned above, most of the empirical models typically include the wind speed only (e.g., Wu, 1988a), in the form

$$W = aU^b. \tag{25}$$

Some of the field observations of whitecap coverage that have the form of Eq. (25) are summarized in Table 1. If we refer to the original observational data sources for these formulas in Table 1, Wu's (1988a) formula is based on observations of Monahan (1971), Toba and Chaen (1973), Monahan *et al*. (1981), Doyle (1984), and Monahan *et al*. (1985); whitecap observations referred to in Hanson and Phillips (1999) are by Monahan and Wilson (1993).

As shown by Eq. (25), these traditional power laws of whitecap coverage correlate only with the wind speed, independent of wave information. This is partly consistent with our inference obtained in Section 2. However, one must wonder why the wind-and-wave-induced processes of whitecapping depend on the wind parameter and not on wave parameters. We note that most of the observations usually exclude any information on wave parameters. To resolve this controversy, we collected observational data of whitecap coverage, which included the information of wind-wave properties, and reanalyzed them by the method of least squares. The data used came from Monahan (1971), Toba and Chaen (1973), Ross and Cardone (1974), and Snyder *et al*. (1983). In order to convert the fetch into the wave parameter, we use the JONSWAP (Hasselmann *et al*., 1973) fetch relationship

$$f_p^* = 3.5X^{-0.33} \tag{26}$$

in the computation, where $f_p^* = Uf_p/g$, $X = gx/U^2$, f_p is the peak frequency, and x the fetch. The drag coefficient $C_D = u_*^2/U^2$ proposed by Wu (1988b) is also applied to convert wind speed into friction velocity as follows

$$C_D = \begin{cases} \left[(1/\kappa)\ln\left(C_D^{1/2}UZ/\nu\right) + 5.5\right]^{-2} & U < 2.4 \text{ m/s} \\ (0.8 + 0.065U)\times 10^{-3} & U > 2.4 \text{ m/s} \end{cases} \tag{27}$$

where $Z = 10$ m is the standard anemometer height, ν the kinematic viscosity of air, and $\kappa = 0.4$ is the Von Kármán constant.

By the method of least squares, we calculated regression of whitecap coverage as a function of wave age β, wave period T_s, wind speed U, friction velocity u_* and breaking-wave parameter R_B, as shown in Figs. 1 to 5, respectively. The regression formulas with the respective correlation coefficients are given in Eqs. (28) to (32):

$$W = 4.69\times 10^{-3}\beta^{1.27} \qquad r = 0.43 \tag{28}$$

$$W = 3.14\times 10^{-2}T_s^{1.82} \qquad r = 0.78 \tag{29}$$

$$W = 2.98\times 10^{-5}U^{4.04} \qquad r = 0.79 \tag{30}$$

$$W = 8.59u_*^{3.42} \qquad r = 0.80 \tag{31}$$

$$W = 3.88\times 10^{-5}R_B^{1.09} \qquad r = 0.88. \tag{32}$$

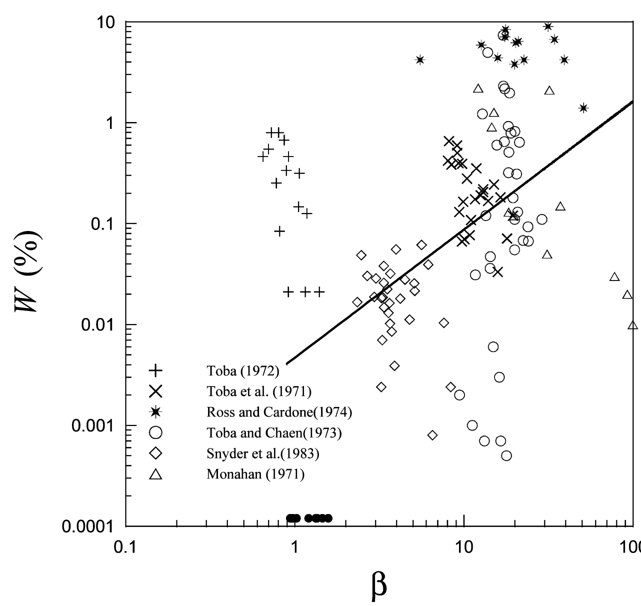

Fig. 1. Whitecap coverage versus wave age $\beta = g/\omega_p u_*$. Data of Toba (1972) and Toba *et al*. (1971) are from a wind-wave tunnel and an oceanographic tower station in a bay, respectively. The other data are from field observations. The solid line can be expressed as $W = 4.69 \times 10^{-3}\beta^{1.27}$ with correlation coefficient of $r = 0.43$. No-whitecapping data ($W = 0$) of Toba (1972) are also denoted by solid circles along the abscissa.

Table 1. Summary of the power-law formulas for whitecap coverage, given in the form of Eq. (25), proposed from in situ observations.

Authors	a ($\times 10^{-6}$)	b
Blanchard (1963)	440	2.0
Monahan (1969)	12	3.3
Monahan (1971)	13.5	3.4
Tang (1974)	7.75	3.23
Wu (1979)	1.7	3.75
Monahan and O'Muircheartaigh (1980)	3.84	3.41
Wu (1988a)	2.0	3.75
Hanson and Phillips (1999)	0.204	3.61

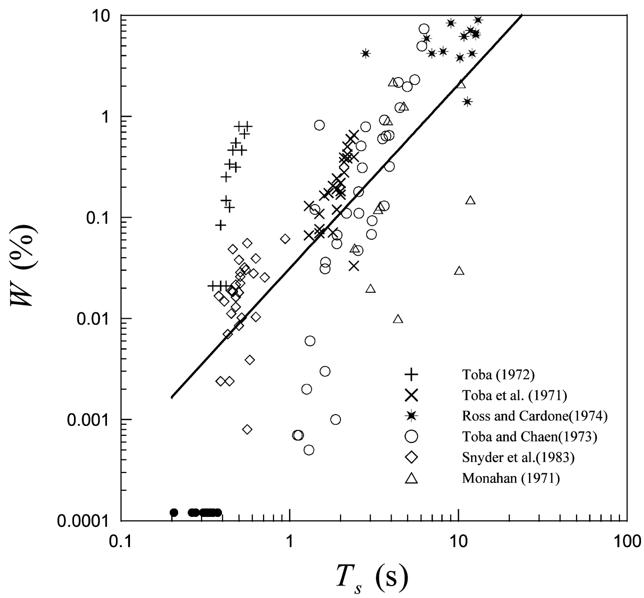

Fig. 2. Whitecap coverage versus the significant wave period T_s. Data source is same as Fig. 1. The solid line can be expressed as $W = 3.14 \times 10^{-2} T_s^{1.82}$ with correlation coefficient of $r = 0.78$. No-whitecapping data ($W = 0$) of Toba (1972) are also denoted by solid circles along the abscissa.

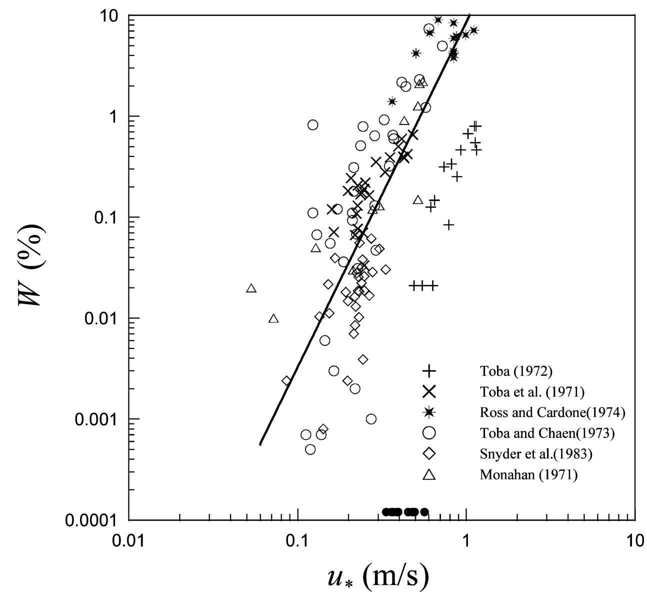

Fig. 4. Whitecap coverage versus friction velocity in the air u_*. Data source is same as Fig. 1. The solid line can be expressed as $W = 8.59 u_*^{3.42}$ with correlation coefficient of $r = 0.80$. No-whitecapping data ($W = 0$) of Toba (1972) are also denoted by solid circles along the abscissa.

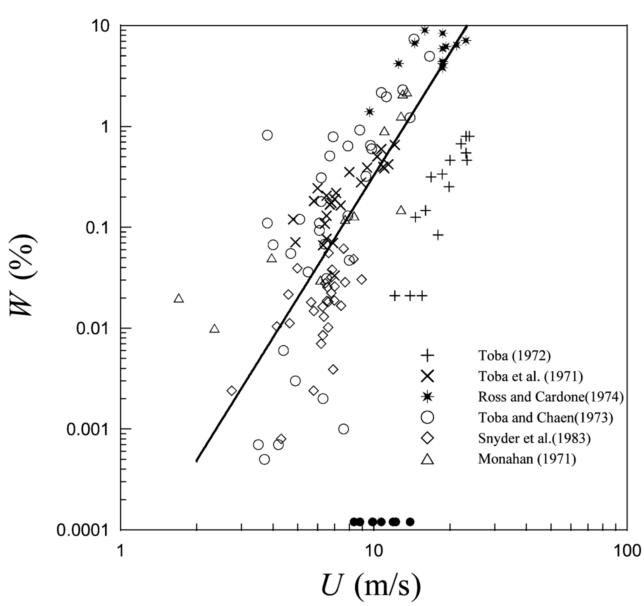

Fig. 3. Whitecap coverage versus wind speed U. Data source is same as Fig. 1. The solid line can be expressed as $W = 2.98 \times 10^{-5} U^{4.04}$ with correlation coefficient of $r = 0.79$. No-whitecapping data ($W = 0$) of Toba (1972) are also denoted by solid circles along the abscissa.

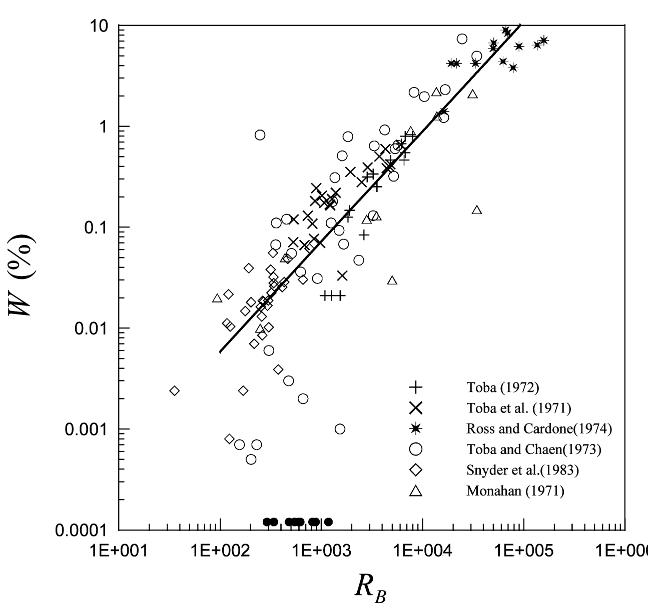

Fig. 5. Whitecap coverage versus breaking wave parameter R_B. Data source is same as Fig. 1. The solid line can be expressed as $W = 3.88 \times 10^{-5} R_B^{1.09}$ with correlation coefficient of $r = 0.88$. No-whitecapping data ($W = 0$) of Toba (1972) are also denoted by solid circles along the abscissa.

In addition, Toba (1972) provided observational data collected in a wind-wave tunnel, and Toba *et al.* (1971) from an oceanographic tower station in a bay, which measured the rate of breaking crests among characteristic wave crests at fixed points. Toba and Koga (1986) reported that these values were able to be converted to whitecap coverage values, with a multiplying factor of 0.021 in their equation (5). For comparison, the converted laboratory data of Toba (1972) and Toba *et al.* (1971) are also added in our figures.

With a correlation coefficient only of 0.43, Eq. (28) shows that, although the wave age has been used to represent the development degree of wind-waves relative to the local winds, it cannot be used to parameterize the whitecap coverage by itself. The data points are naturally separated in the abscissa values from laboratory to tower and to open sea data groups. From Eq. (29), one can see that wave period correlates better with the data than does the wave age. Compared with the wave parameter shown in Figs. 1 and 2, the wind parameters correlate with the whitecap coverage a little better as shown in Figs. 3 and 4. This may be why the traditional power laws of whitecap coverage were expressed in terms of the wind speed, not of the wave height or the wave period. However, one can still see a trend similar to that seen in Figs. 1 and 2, though the trend is in the opposite direction in the abscissa values.

As shown in Fig. 5, however, the breaking-wave parameter R_B proposed by Toba and Koga (1986), which is a parameter combining wind and wind-wave properties, describes the whitecap coverage best, with much smaller data scatter. Laboratory and field data collapse on a straight line with almost 45° slope. Furthermore, our results also confirm the conclusion of Toba and Koga (1986) that wind-wave breaking will occur when R_B exceeds about 10^3. Therefore, the breaking-wave parameter is preferred in describing whitecap coverage. A physical interpretation of R_B is given in Section 5.

We note that R_B can be rewritten as

$$R_B = (g\nu)^{-1} u_*^3 \beta. \tag{33}$$

In addition to the correlation with the cube of friction velocity, Eq. (33) clearly demonstrates a stronger dependence of W on wave age than the ideas indicated by formulas such as Wu (1988a), and by the two theoretical models for wind-wave dissipation. It is inferred that the current dissipation models have at least not addressed full properties and should be modified further to take account of the wind-wave parameters.

We noted that, in Figs. 1 to 4, the laboratory data always had some systematic deviations from the field data, meaning that they cannot be reconciled by the parameters used in preparing these figures. In Fig. 5, however, when we use R_B, the laboratory data are very consistent with the field data. If the regression results including and excluding the tower station data of Toba *et al.* (1971) and laboratory data of Toba (1972) are compared, all of the correlation coefficients will be significantly reduced in the case including these data, with the exception of the case of R_B. In this case, the correlation coefficient changes little around $r = 0.87$ (Table 2). This demonstrates that R_B is a suitable parameter for describing the overall conditions of air-sea boundary processes, as Toba and Koga (1986) inferred.

Table 2. Comparison of correlation coefficients for various parameters shown in Figs. 1–5.

	Excluding lab. data	Including lab. data
β	0.43	0.21
T_s	0.78	0.65
U	0.79	0.69
u_*	0.80	0.70
R_B	0.88	0.87

In order to further confirm our conclusion, we should have a much larger data set in the analysis, especially observations including wave information. However, it is usually difficult to obtain this kind of data in severe conditions, such as under typhoons and hurricanes, where large-scale wind-wave breaking occurs and plays a key role in the air-sea boundary processes. This weakness would be eliminated in the future if, with the development of remote sensing technology, satellite data could be used to obtain the information on wave breaking under such conditions.

4. Probability Models of Whitecap Coverage

There is a view that the surface waves at the sea surface are composed of water waves, in which the very local wind forcing is not necessarily considered. From such a viewpoint, Snyder *et al.* (1983) estimated whitecap coverage analytically in terms of an acceleration criterion. Ochi and Tsai (1983) examined the prediction of breaking occurrence in deep water using a breaking criterion of wave steepness for individual waves. To avoid computations of higher order moments of wave spectra, these kinds of studies are based on linear wave theory, in which the wave characteristics, such as surface elevations, surface slope and surface acceleration, are Gaussian according to the central limit theorem of probability. Therefore, the probability density function of random surface elevation, $\eta(\vec{x}, t)$, can be expressed as

$$P(\eta) = \frac{1}{\sqrt{2\pi m_0}} \exp\left(-\frac{\eta^2}{2m_0}\right) \quad (34)$$

and

$$m_0 = \langle \eta^2 \rangle \equiv \int \Phi(\omega) d\omega \quad (35)$$

where $\langle\ \rangle$ denotes an ensemble average and m_0 is the 0-th moment of wave spectrum $\Phi(\omega)$; the n-th moment is defined as

$$m_n = \int_0^\infty \omega^n \Phi(\omega) d\omega. \quad (36)$$

For wave steepness criterion of wave breaking, the wave slope can be defined as

$$\eta_s = \frac{d\eta}{dx} \equiv \frac{d\eta}{dt}\frac{dt}{dx} = -\frac{\omega}{c}\eta = -\frac{1}{g}\omega^2 \eta \quad (37)$$

where $c = g/\omega$ is the phase speed. The probability density function of the wave slope can thus be written as

$$P(\eta_s) = \frac{g}{\sqrt{2\pi m_4}} \exp\left(-\frac{g^2 \eta_s^2}{2m_4}\right) \quad (38)$$

and

$$m_4 = \int \omega^4 \Phi(\omega) d\omega. \quad (39)$$

For the wave surface acceleration criterion of wave breaking, the surface acceleration can be defined as

$$\eta_{tt} = \frac{d^2\eta}{dt^2} = \omega^2 \eta. \quad (40)$$

In the same way, the probability density function of wave surface acceleration can be written as

$$P(\eta_{tt}) = \frac{1}{\sqrt{2\pi m_4}} \exp\left(-\frac{\eta_{tt}^2}{2m_4}\right). \quad (41)$$

Assume that the wave surface will break where the wave slope exceeds a threshold, γ_s, for the slope criterion, and where the surface acceleration exceeds a threshold, $\gamma_{tt} g$, for the acceleration criterion. From Eqs. (38) and (41), the probability of wave breaking, which is equivalent to whitecap coverage (Snyder *et al.*, 1983), can be calculated as

$$W_s = \int_{\gamma_s}^\infty P(\eta_s) d\eta_s = 1 - \varphi\left(\frac{\gamma_s g}{m_4^{1/2}}\right) \quad (42)$$

$$W_{tt} = \int_{\gamma_{tt} g}^\infty P(\eta_{tt}) d\eta_{tt} = 1 - \varphi\left(\frac{\gamma_{tt} g}{m_4^{1/2}}\right) \quad (43)$$

$$\varphi(z) = \frac{1}{\sqrt{2\pi}} \int_{-\infty}^z e^{-y^2/2} dy. \quad (44)$$

We note that no matter what kind of threshold is used to determine wave breaking, they give the same results of wave breaking probability, which depend on the fourth moment of the wave spectrum and the chosen threshold.

The fundamental dilemma of the probability model is that the strongly nonlinear process of wave breaking could be characterized by those relationships based on linear wave theory, apart from further nonlinear processes of wind forcing. Even if we ignore this dilemma, there are still some practical difficulties in estimating m_4 and determining γ_s or γ_{tt} because m_4 is theoretically indeterminable by the wave spectra characterized by the Phillips equilibrium range, and the values of γ_s and γ_{tt} are quite variable in both theory and experiment. The equilibrium range expressed by Eq. (4) was reached by inclusion of the effect of wind forcing (Phillips, 1985).

In general, the wave breaking criterion, wave slope or acceleration, is considered as constant (Longuet-Higgins, 1963; Ochi and Tsai, 1983; Kennedy and Snyder, 1983; Xu *et al.*, 2000), so W depends completely on m_4. To prevent m_4 from being indeterminable, we must employ some approximation methods in the estimation, such as adopting the spectral cutoff (Snyder *et al.*, 1983) or time averaging (Glazman, 1986). Using the latter method and their observational data, Xu *et al.* (2000) derived m_4 as follows

$$m_4 = 1.22 g^2 X^{-0.5} \quad (45)$$

$$X = gx / U^2 \quad (46)$$

where X is a nondimensional fetch and x is a fetch. Letting $\gamma_{tt} = 0.3$, W_{tt} can be expressed as

$$W_{tt} = 1 - \varphi\left(0.29 X^{0.25}\right) \quad (47)$$

from Eq. (43). This formula, proposed by Xu *et al.* (2000), predicts that the whitecap coverage can be parameterized

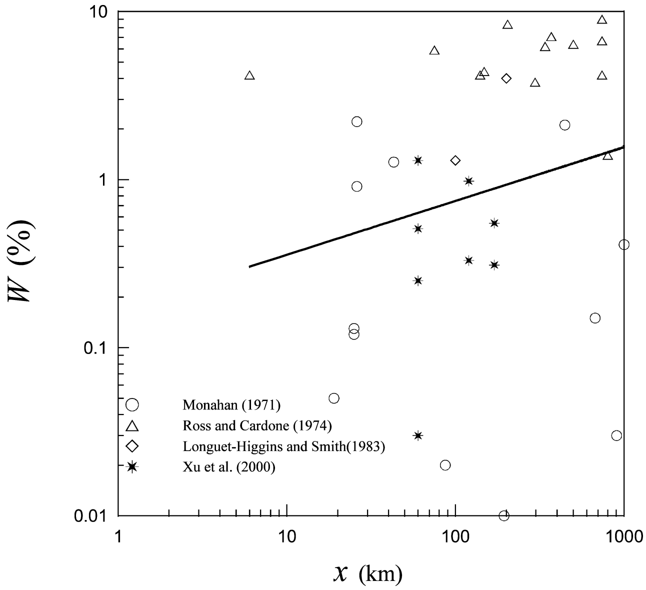

Fig. 6. Whitecap coverage as a function of fetch x (km) found by reanalyzing previous field observations of Monahan (1971), Ross and Cardone (1974), Longuet-Higgins and Smith (1983) and Xu *et al*. (2000).

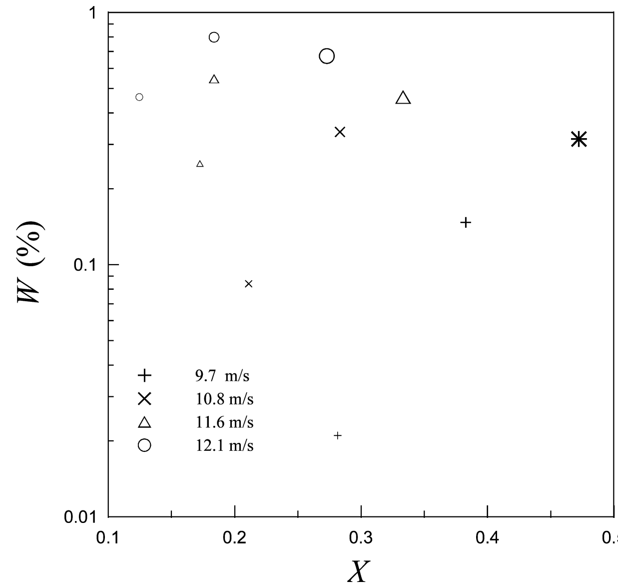

Fig. 8. Observational data of Toba (1972) from a wind-wave tank are plotted by nondimensional fetch $X = gx/U^2$. The symbols of +, ×, △ and ○ indicate the mean wind speeds in the tunnel section 9.7, 10.8, 11.6, and 12.1 m/s, respectively. The symbols in small, medium and large sizes denote the fetch of 6.9, 10.0 and 13.6 m, respectively.

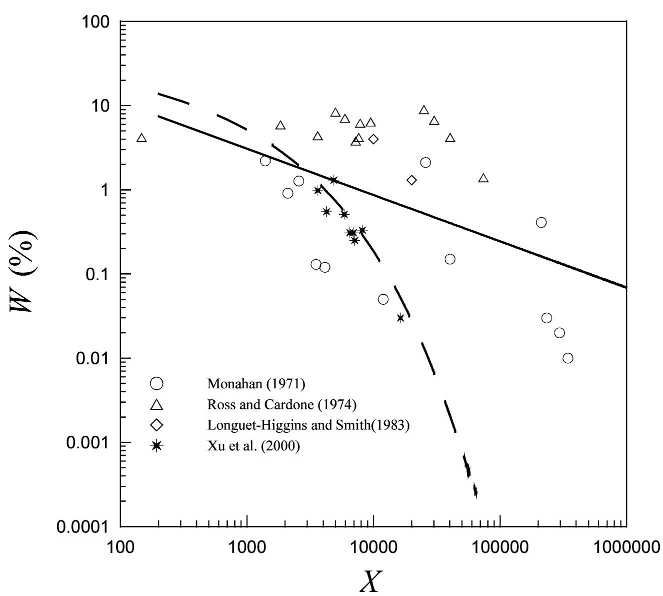

Fig. 7. Whitecap coverage as a function of nondimensional fetch $X = gx/U^2$ by reanalyzing previous field observations of Monahan (1971), Ross and Cardone (1974), Longuet-Higgins and Smith (1983) and Xu *et al*. (2000). The solid line is obtained by the method of least squares. The dashed line is the formula proposed by Xu *et al*. (2000).

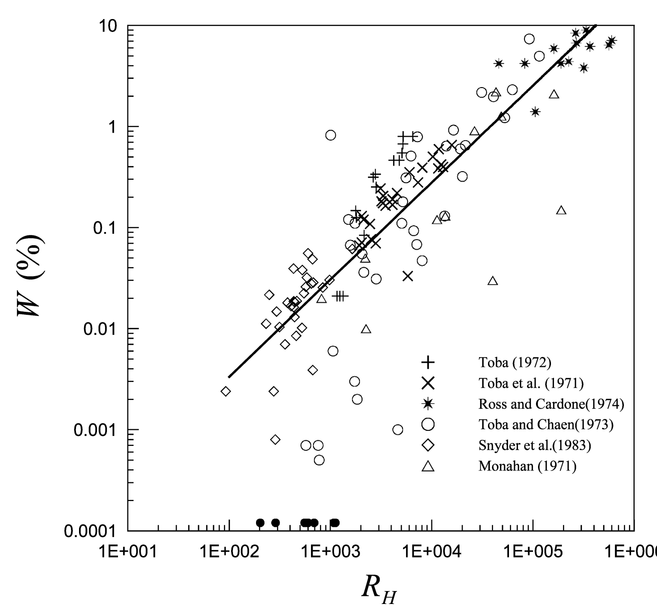

Fig. 9. Whitecap coverage versus nondimensional parameter R_H. Data source is same as Fig. 1. The solid line can be expressed as $W = 4.02 \times 10^{-5} R_B{}^{0.96}$ with correlation coefficient of $r = 0.84$. No-whitecapping data ($W = 0$) of Toba (1972) are also denoted by solid circles along the abscissa.

by a nondimensional fetch and will become smaller with increasing X. Equation (47) seems to contradict Eq. (32) because Eq.(26) shows that β is equivalent to X.

To clarify this discrepancy, we collected some previous field observations of whitecap coverage that includes fetch information and reanalyzed the data by the method of least squares. Whitecap coverage as a function of fetch x and nondimensional fetch X is shown in Figs. 6 and 7. With the method of least squares, whitecap coverage can be characterized by x and X as

$$W = 0.171x^{0.32} \qquad r = 0.21 \tag{48}$$

$$W = 137.3X^{-0.55} \qquad r = 0.46. \tag{49}$$

Equations (48) and (49) are also plotted in Figs. 6 and 7. Equation (47) is also plotted on Fig. 7 as a dashed line for comparison.

At first, with such a low correlation coefficient, it is clear that one cannot parameterize whitecap coverage by using fetch or nondimensional fetch only. As we mentioned above, the wave-breaking process is strongly related with the wind forcing, or the wind speed, and one can only add other parameters to decrease data scatter but cannot completely replace it with other parameters such as T_s, β, x, or X. It is therefore not good enough to use Eq. (47) to represent the properties of wave breaking, though it agrees well with the data of Xu *et al*. (2000).

Another contradiction is why the inclinations of W on fetch are opposed when using x and X as shown in Eqs. (48) and (49). Although the wave age is usually regarded as a parameter equivalent to X from Eq. (26), we should use X with caution in real applications. Limited by the severe conditions in the field, the wave observations are usually conducted at a fixed fetch, while the changeable factor is the wind. In this case, the change of X is just a reflection of the variability of U, and not of x. As W is clearly increasing with U, while $X \propto U^{-2}$, this leads to the minus index in Eq. (49). Therefore, the fact that W decreases with increasing X, as shown in Eqs. (47) and (49), reflects the fact that W depends closely on U. This is also clearly shown in Fig. 8, in which laboratory data of Toba (1972) are plotted against X. The same kind of symbols indicate the situations of changeable fetch with constant mean wind speed, and the same size of symbols denote the situations of changeable mean wind speed with constant fetch. For the former W is increasing with X, while for the latter W is decreasing with X.

Many studies are also inconsistent with the intuitive notion that the onset of wave breaking occurs at some critical geometrical or dynamical values, as mentioned above. For example, Holthuijsen and Herbers (1986) in their detailed study of wave breaking in the open ocean reported that it was difficult to distinguish the population of breaking waves from the overall wave population on the basis of their steepness probability distributions. Through numerical simulation, Tulin and Li (1992) concluded that significant differences in energy existed along the wave group, particularly between the trough and crest regions of the steepest wave near the center of the wave group. Wang *et al.* (1993) confirmed this idea and suggested that a threshold for determining breaking onset involved the ratio of horizontal water speed at the crest to the group velocity. They found that for all cases that proceeded to breaking, this ratio exceeded one. Schultz *et al.* (1994) suggested an absolute criterion of potential energy/total wave energy exceeding 0.52. On the other hand, the numerical simulation study of Banner and Tian (1998) provided evidence for the existence of a threshold of the local relative growth rates of the mean wave momentum and energy density, which had been investigated widely by observations (e.g., Snyder *et al*., 1981; Plant, 1982; Mitsuyasu and Honda, 1982). They indicated that wave breaking occurs when these relative growth rates are sustained at the threshold of 0.2.

As a summary, the direct application of probability theory with a universal surface criterion, such as γ_s or γ_{tt}, is very ambiguous, even in the case of wind-waves in local equilibrium with the wind, as questioned by Banner and Tian (1998). Naturally, it is impossible to use this kind of wave parameter to describe wave-breaking behavior in more complicated situations, such as shoaling and multi-directional wave fields.

5. Physical Interpretation of Breaking-Wave Parameter R_B and Some Related Issues

In Section 3 we demonstrated that the breaking-wave parameter R_B can parameterize the past data set of whitecap coverage or wind-wave breaking very well. The wind speed, the air-friction velocity, and wave parameters are not by themselves well correlated with these data. In this section we discuss the physical interpretation of R_B and its limitation in applicability.

Wind waves are very special phenomena, which are generated at a shear (frictional) interface between the air and water, and which connect two turbulent boundary layers of air and water. Swells can be expressed rather well by a superposition of Fourier components of small amplitudes. On the contrary, pure wind generated waves have special characteristics which may not be expressed by linear superposition of component waves. In case of these pure wind-waves, there exist similarity laws, such as a similarity spectral form expressed by Eq. (4) on its high frequency side (this is the equilibrium range), and the 3/2-power law Eq. (16) between characteristic wave height and period in nondimensional forms. In other words, for wind-waves free of swells, wave height and period of individual waves (see e.g., Toba, 1978; Tokuda and Toba, 1981) cannot adopt arbitrary values, but are combined statistically with each other under wind forcing as expressed by u_*. This situation is created by the strongly nonlinear self-adjustment processes between the local wind and the wind-wave field. This is a concept of the "wind-waves in local equilibrium with the wind". A comprehensive review of this issue was given in Toba (1998).

Under the existence of swells, the equilibrium range of Eq. (4) still exists for the wind-wave part (e.g., Hanson and Phillips, 1999). Also, the 3/2-power law seems highly robust under the existence of some swells that are not dominant (e.g., Kawai *et al.*, 1977). The 3/2-power law holds in strong winds or high seas, e.g., for situation of $H_s > 4$ m as demonstrated by Ebuchi *et al.* (1992). We may thus express the situation of wind-waves under the effective action of the wind by u_* together with either of H_s, T_s or ω_p.

The breaking-wave parameter R_B is a nondimensional number composed of u_*, ω_p, and the kinematic viscosity of air ν. Toba and Koga (1986) gave the following interpretation. The inverse of the peak angular frequency, $\omega_p^{-1} = T/2\pi$, represents π^{-1} times the time interval, $(T/2)$, required for a fixed water surface point to reach the top of a crest from the bottom of a trough, or vice versa. If we consider a length scale $L = u_*(T/2\pi)$, which relates to the recirculation (see e.g., Ebuchi *et al.*, 1993), then R_B may be interpreted as a kind of Reynolds number u_*L/ν, which may have a threshold value of the order of 10^3, as in the case of the turbulent Reynolds number that is usually employed. The inclusion of viscosity is natural since, in the breaking at a wind forced wave surface with recirculation cap at the crest, the viscosity should play a significant role in forming such a criterion as the Reynolds number. The existence of the equilibrium range spectral form Eq. (4) during the downshifting of the peak frequency in the wind-wave growth processes seems to indicate necessity of a viscosity term in the wind-wave processes throughout the continuous high-frequency spectral range. The absolute value of this threshold is not definite, theoretically. However, the value of about 10^3 corresponds well to the observed condition of the onset of wave breaking, whitecapping, and sea spray production, as demonstrated in Fig. 5 of the present paper, figures 2 and 3 of Toba and Koga (1986), and figure 3 of Iida *et al.* (1992).

The typical length scale to construct Reynolds number is ambiguous. We can use another length scale such as the thickness of the downward bursting turbulent boundary layer (DBBL) of $5H_s$, which Toba and Kawamura (1996) proposed experimentally, or just H_s, instead of the above length scale L. In this case, another Reynolds number can be defined by $R_H = u_*H_s/\nu$. The same data as Fig. 5 are plotted in Fig. 9 using R_H as the abscissa. The data point scatter is very similar to Fig. 5, with a slightly smaller correlation coefficient of $r = 0.84$. The regression line with respect to R_H can be expressed as

$$W = 4.02 \times 10^{-5} R_H^{0.96}. \tag{50}$$

In fact, R_H and R_B can be mutually related by the following equation by using the 3/2-power law without any other independent quantity in the case of wind-waves in local equilibrium with the wind, with $B = 0.062$ as a constant of the 3/2-power law:

$$R_H = B\left(\frac{2\pi}{1.05}\right)^{3/2} \beta^{1/2} R_B. \tag{51}$$

Also, we can use the kinematic viscosity of water ν_w (of the order of 0.015 cm^2/s) instead of the kinematic viscosity of air ν (of the order of 0.15 cm^2/s). The former might be better conceptually in defining the wave breaking criterion. However, both of these viscosities are physical constants at the air-water boundary, and the ratio between them is a constant, so they will only give a difference in the absolute values for the threshold criterion. Since the selection of these Reynolds numbers is arbitrary, we will use the original R_B which Toba and Koga (1986) proposed.

Banner *et al.* (2000) analyzed field observation data in the Black Sea and Lake Washington, and found that the dominant breaking wave probability is strongly correlated with the significant spectral peak steepness, defined by

$$\varepsilon = \frac{H_p \omega_p^2}{2g} \tag{52}$$

where

$$H_p = \left\{\int_{0.7\omega_p}^{1.3\omega_p} \Phi(\omega)d\omega\right\}^{1/2},$$

and $\Phi(\omega)$ the frequency spectrum of the windsea after filtration of any background swell. They found that the probability of breaking is zero, up to a threshold value of $\varepsilon = 0.055$, and then increases close to quadratically for $\varepsilon > 0.055$ with a correlation coefficient of 0.78. This steepness, however, was found to have a unique relation with the wave age according to the 3/2-power law, as shown by Bailey *et al.* (1991), for wind waves in local equilibrium with the wind. In this case the wind forcing parameter R_B should be more appropriate, as indicated in the present paper.

As discussed above, the effectiveness of R_B is confined to the wind forced situation, although the existence of some non-dominant natural swells is allowed. However, there are many other cases of wave breaking in the sea. For example, the waves can break in the total absence of wind (e.g., Dold and Peregrine, 1986; Rapp and Melville, 1990) due to inherent hydrodynamic processes in water. There are also conditions of enhanced wave dissipation due to the up-current propagation or due to shoaling, or in multi-directional wave fields. In these cases the wind-forced R_B parameterization will not be applicable, and a hydrodynamic parameter characterizing inherent wave field will be preferred, as is also discussed in Banner *et al.* (2000).

6. Conclusions

The wave breaking is believed to play a key role in air-sea boundary processes. In order to estimate the effects caused by whitecaps, we must describe the process quantitatively. However, the wave-breaking process is highly nonlinear, and it is very difficult to investigate, both theoretically and experimentally. Very few quantitative methods are available to accomplish this. In wave prediction theory, the dissipation source term has been given explicitly. By using the equilibrium spectrum and the field observations, we calculate the total rate of wave energy dissipation based on the dissipation models proposed by Hasselmann (1974) and Phillips (1985). Although the two models differ significantly in their forms, the total rates of wind-wave energy obtained from them mainly depend on the cube of the air friction velocity, and are affected little by the wave age.

Another quantitative way to describe wave breaking is by whitecap coverage, which is directly proportional to the total rate of wave energy dissipation because it describes the same process but in a visible manifestation. One may thus infer that whitecap coverage should be proportional to the cube of the air friction velocity. This explains why previous typical power law formulas for whitecap coverage usually employ only wind speed, in spite of the fact that the wave breaking is a phenomenon involving coupling between wind and waves. Reanalysis of previous observational data of whitecaps has confirmed this inference. It is found that the traditional approach of relating whitecap coverage to the wind speed or to the air friction velocity provides a better correlation than relating it to such wave parameters as wave period or wave age.

However, compared with wind parameters, the data scatter decreased remarkably by employing the breaking-wave parameter R_B proposed by Toba and Koga (1986). The parameter R_B can be interpreted as one kind of Reynolds number, which characterizes the wave breaking behavior for the case where wind-waves are effectively in local equilibrium with the wind, and where the wave height and wave period are combined statistically as expressed by the 3/2-power law. R_B also provides a threshold criterion for the onset of whitecapping or sea spray production. Namely, whitecaps occur when R_B is greater than 10^3. We thus conclude that R_B is the best parameter now available to be used to parameterize the wave-breaking process.

Since R_B can be expressed as the product of the cube of friction velocity and wave age, whitecap coverage depends partly on wave age. The fact that R_B allows us to reconcile the diverse data set from the laboratory to the field implies that the well-controlled laboratory results could be applied to the field with parameterization by R_B. This point is very important because the laboratory studies are indispensable to understanding the mechanism of various wave-breaking related phenomena involved in the air-sea boundary processes.

It is noted that ocean waves can break without wind forcing by inherent hydrodynamic processes in water, such as wave current interactions and shoaling. Applications of the present results are thus limited to the effective wind forcing situations, where the 3/2-power law is satisfied.

Finally, we suggest that the wind-wave dissipation models should also be modified in a manner to reflect the full properties involved in the wave-breaking processes.

Acknowledgements

The author D. Zhao expresses his thanks to the Science and Technology Agency of Japan for providing him with the STA fellowship. The authors thank two anonymous reviewers for their valuable comments leading to improvement in our original manuscript.

References

Bailey, R. J., I. S. F. Jones and Y. Toba (1991): The steepness and shape of wind waves. *J. Oceanogr. Soc. Japan*, **47**, 249–264.

Banner, M. L. and X. Tian (1998): On the determination of the onset of wave breaking for modulating surface gravity water waves. *J. Fluid Mech.*, **367**, 107–137.

Banner, M. L., A. V. Babanin and I. R. Young (2000): Breaking probability for dominant waves on the sea surface. *J. Phys. Oceanogr.*, **30**, 3145–3160.

Blanchard, D. C. (1963): The electrification of the atmosphere by particles from bubbles in the sea. *Progress in Oceanography*, Vol. 1, Pergamon Press, 71–202.

Cardone, V. J. (1970): *Specification of the Wind Distribution in the Marine Boundary Layer for Wave Forecasting*. New York University, 131 pp.

Dold, J. W. and D. H. Peregrine (1986): Water-wave modulations. *Proceedings of the 20th International Conference on Coastal Engineering*, ASCE, Taipei, **1**, 163–165.

Donelan, M. A., M. Skafel, H. Graber, P. Liu, D. Schwab and S. Venkatesh (1992): On the growth rate of wind-generated waves. *Atmos.-Ocean*, **30**, 457–478.

Doyle, D. M. (1984): Marine aerosol research in the Gulf of Alaska and on the Irish West Coast (Inishmore). *Whitecaps and the Marine Atmosphere Rep. 6*, University College, Galway, Ireland.

Ebuchi, N., Y. Toba and H. Kawamura (1992): Statistical study on the local equilibrium between wind and wind waves by using data from ocean data buoy stations. *J. Oceanogr.*, **48**, 77–92.

Ebuchi, N., H. Kawamura and Y. Toba (1993): Bursting phenomena in the turbulent boundary layer beneath the laboratory wind-wave surface. p. 263–276. In *Natural Physical Sources of Underwater Sound*, ed. by B. Kerman, Kluwer Acad. Pub.

Felizardo, F. C. and W. K. Melville (1995): Correlations between ambient noise and the ocean surface wave field. *J. Phys. Oceanogr.*, **25**, 513–532.

Glazman, R. E. (1986): Statistical characteristics of sea surface geometry for a wave slope field discontinuous in the mean square. *J. Geophys. Res.*, **91**, 6629–6641.

Glazman, R. E. and A. Greysukh (1993): Satellite altimeter measurements of surface wind. *J. Geophys. Res.*, **98**, 2475–2483.

Hanson, J. L. and O. M. Phillips (1999): Wind sea growth and dissipation in the open ocean. *J. Phys. Oceanogr.*, **29**, 1633–1648.

Hasselmann, K. (1974): On the spectral dissipation of ocean waves due to whitecapping. *Bound.-Layer Meteor.*, **126**, 107–127.

Hasselmann, K. and 15 authors (1973): Measurements of wind wave growth and swell decay during the Joint North Sea Wave Project (JONSWAP). *Dt. Hydrogr. Z.*, **A8**(22), 95 pp.

Holthuijsen, L. H. and T. H. C. Herbers (1986): Statistics of breaking waves observed as whitecaps in the open sea. *J. Phys. Oceanogr.*, **16**, 290–297.

Iida, N., Y. Toba and M. Chaen (1992): A new expression for the production rate of sea water droplets on the sea surface. *J. Oceanogr.*, **48**, 439–460.

Kawai, S., K. Okada and Y. Toba (1977): Field data support of three seconds power law and the $gu_*\sigma^{-4}$-spectral form for growing wind waves. *J. Oceanogr. Soc. Japan*, **33**, 137–150.

Kennedy, R. M. (1992): Sea surface dipole sound source dependence on wave-breaking variables. *J. Acoust. Soc. Amer.*, **91**, 1974–1982.

Kennedy, R. M. and R. L. Snyder (1983): On the formation of whitecaps by a threshold mechanism. Part II: Monte Carlo experiments. *J. Phys. Oceanogr.*, **13**, 1493–1504.

Komen, G. J., S. Hasselmann and K. Hasselmann (1984): On the existence of a fully developed wind-sea spectrum. *J. Phys. Oceanogr.*, **14**, 1271–1285.

Longuet-Higgins, M. S. (1963): The generation of capillary waves by steep gravity waves. *J. Fluid Mech.*, **16**, 138–159.

Longuet-Higgins, M. S. and N. D. Smith (1983): Measurement of breaking waves by a surface meter. *J. Geophys. Res.*, **88**, 9823–9831.

Mitsuyasu, H. and T. Honda (1982): Wind-induced growth of water waves. *J. Fluid Mech.*, **123**, 425–442.

Mitsuyasu, H., F. Tasai, T. Suhara, S. Mizuno, M. Ohkusu, T. Honda and K. Rikiishi (1980): Observation of the power spectrum of ocean waves using a clover-leaf buoy. *J. Phys. Oceanogr.*, **10**, 286–296.

Monahan, E. C. (1969): Fresh water whitecaps. *J. Atmos. Sci.*, **26**, 1026–1029.

Monahan, E. C. (1971): Oceanic whitecaps. *J. Phys. Oceanogr.*, **1**, 139–144.

Monahan, E. C. and I. G. O'Muircheartaigh (1980): Optimal power-law description of oceanic whitecap coverage dependence on wind speed. *J. Phys. Oceanogr.*, **10**, 2094–2099.

Monahan, E. C. and I. G. O'Muircheartaigh (1982): Reply. *J. Phys. Oceanogr.*, **12**, 751–752.

Monahan, E. C. and M. Wilson (1993): Whitecap measurements. Critical Sea Test 7, Phase 2: Principal investigators' results. *The Johns Hopkins University Applied Physics Laboratory Tech. Rep. STD-R-2258*, ed. by F. T. Erskine and J. L. Hanson, 808 pp.

Monahan, E. C., I. G. O'Muircheartaigh and M. P. Fitzgerald (1981): Determination of surface wind speed from remotely measured whitecap coverage, a feasibility assessment. *European Space Agency SP-167*, 103–109.

Monahan, E. C., P. A. Bowyer, D. M. Doyle, M. R. Higgins and D. K. Woolf (1985): Whitecaps and the marine atmosphere. *Whitecaps and the Marine Atmosphere Rep. 8*, University College, Galway, Ireland.

Ochi, M. K. and C. H. Tsai (1983): Prediction of occurrence of breaking waves in deep water. *J. Phys. Oceanogr.*, **13**, 2008–2019.

Phillips, O. M. (1985): Spectral and statistical properties of the equilibrium range in wind-generated gravity waves. *J. Fluid Mech.*, **156**, 505–531.

Plant, W. J. (1982): A relationship between wind stress and wave slope. *J. Geophys. Res.*, **87**(C3), 1961–1967.

Rapp, R. J. and W. K. Melvill (1990): Laboratory measurements of deep-water breaking waves. *Phil. Trans. R. Soc. Lond.*, **A331**, 735–800.

Ross, D. B. and V. Cardone (1974): Observations of oceanic whitecaps and their relation to remote measurements of surface wind speed. *J. Geophys. Res.*, **79**, 444–452.

Schultz, W. W., J. Huh and O. M. Griffin (1994): Potential energy in steep and breaking waves. *J. Fluid Mech.*, **278**, 201–228.

Snyder, R. L., F. W. Dobson, J. A. Elliott and R. B. Long (1981): Array measurements of atmospheric pressure fluctuations above surface gravity waves. *J. Fluid Mech.*, **102**, 1–59.

Snyder, R. L., L. Smith and R. M. Kennedy (1983): On the formulation of whitecaps by a threshold mechanism. Part III: Field experiment and comparison with theory. *J. Phys. Oceanogr.*, **13**, 1505–1518.

Tang, C. C. H. (1974): The effect of droplets in the air-sea transition zone on the sea brightness temperature. *J. Phys. Oceanogr.*, **4**, 579–593.

Toba, Y. (1972): Local balance in the air-sea boundary processes. I. On the growth processes of wind waves. *J. Oceanogr. Soc. Japan*, **28**, 109–120.

Toba, Y. (1973): Local balance in the air-sea boundary processes. III. On the spectrum of wind waves. *J. Oceanogr. Soc. Japan*, **29**, 209–220.

Toba, Y. (1978): Stochastic form of the growth of wind waves in a single-parameter representation with physical implications. *J. Phys. Oceanogr.*, **8**, 494–507.

Toba, Y. (1998): Wind-forced strong wave interactions and quasi-local equilibrium between wind and windsea with the friction velocity proportionality. p. 1–60. In *Nonlinear Ocean Waves*, ed. by W. Perrie, Computational Mechanics Publications, Southampton, U.K.

Toba, Y. and M. Chaen (1973): Quantitative expression of the breaking of wind waves on the sea surface. *Rec. Oceanogr. Works Japan*, **12**, 1–11.

Toba, Y. and H. Kawamura (1996): Wind-wave coupled downward-bursting boundary layer (DBBL) beneath the sea surface. *J. Oceanogr.*, **52**, 409–419.

Toba, Y. and M. Koga (1986): A parameter describing overall conditions of wave breaking, whitecapping, sea-spray production and wind stress. p. 37–47. In *Oceanic Whitecaps*, ed. by E. C. Monahan and G. Mac Niocaill, Reidel Publishing Company.

Toba, Y., H. Kunishi, K. Nishi, S. Kawai, Y. Shimada and N. Shibata (1971): Study on the air-sea boundary processes at the Shirahama Oceanographic Tower Station. *Disacs. Prev. Res. Inst. Kyoto Univ., Annals*, **14B**, 519–531 (in Japanese with English abstract).

Toba, Y., S. Kizu and N. Ebuchi (1988): On-board quantitative wind-wave observations using a stop watch. *Prel. Rep. of The Hakuho Maru Cruise KH-88-2 (OMLET Cruise)*, Ocean Res. Inst., Univ. of Tokyo, 35–44.

Toba, Y., Y. Suzuki and N. Iida (1999): Study on global distribution with seasonal variation of the whitecap coverage and sea-salt aerosol production on the sea surface. p. 355–356. In *The Wind-Driven Air-Sea Interface*, ed. by M. L. Banner, School of Mathematics, The University of New South Wales, Sydney, Australia.

Tokuda, M. and Y. Toba (1981): Statistical characteristics of individual waves in laboratory wind waves. I. Individual wave spectra and similarity structure. *J. Oceanogr. Soc. Japan*, **37**, 243–258.

Tulin, M. P. and J. J. Li (1992): On the breaking of energetic waves. *J. Intl. Soc. Offshore and Polar Engng.*, **2**, 46–53.

WAMDI Group (1988): The WAM model—A third generation ocean wave prediction model. *J. Phys. Oceanogr.*, **18**, 1775–1810.

Wang, P., Y. Yao and M. P. Tulin (1993): Wave group evolution, wave deformation and breaking simulations using LONGTANK, a numerical wave tank. *Proc. 3rd Intl. Offshore and Polar Engng Conf.*, Singapore, Vol. 27.

Wu, J. (1979): Oceanic whitecaps and sea state. *J. Phys. Oceanogr.*, **9**, 1064–1068.

Wu, J. (1982): Comments on “Optimal power-law description of oceanic whitecap coverage dependence on wind speed”. *J. Phys. Oceanogr.*, **12**, 750–751.

Wu, J. (1988a): Variations of whitecap coverage with wind stress and water temperature. *J. Phys. Oceanogr.*, **18**, 1448–1453.

Wu, J. (1988b): Wind-stress coefficients at light winds. *J. Atmos. Oceanic Technol.*, **5**, 885–888.

Xu, D., X. Liu and D. Yu (2000): Probability of wave breaking and whitecap coverage in a fetch-limited sea. *J. Geophys. Res.*, **105**, 14253–14259.